A Novel Assessment of the Vertical Velocity Correction for Non-orthogonal Sonic Anemometers

Kyaw Tha Paw U[1], Mary Rose Mangan[1,2], Jilmarie Stephens[1,a], Kosana Suvočarev[1], Jenae' Clay[1], Olmo Guerrero Medina[1], Emma Ware[1], Amanda Kerr-Munslow[3], James McGregor[3], John Kochendorfer[1,b], Megan McAuliffe[1,c], Megan Metz[1,d]

[1] Atmospheric Science, University of California, Davis, CA 95616 USA
[2] Meteorology and Air Quality Group, Wageningen University, Droevendaalsesteeg 3a, 6708 PB Wageningen, the Netherlands
[3] Field Site Cardington Airfield, Met Office, Bedford MK42 0SY, United Kingdom
[a] now at Cooperative Institute for Research in Environmental Sciences, University of Colorado, Boulder, CO 80309 USA
[b] now at Atmospheric Turbulence and Diffusion Division, NOAA Air Resources Laboratory, Oak Ridge, TN 37830 USA
[c] now at Triangulum Insights, Inc., Willmar, MN 56201 USA
[d] now at Cropping Systems and Water Quality Research, USDA Agricultural Research Service, Columbia, MO 65211 USA

Correspondence to: Kyaw Tha Paw U (ktpawu@ucdavis.edu)

Abstract. Non-orthogonal sonic anemometers are used extensively in flux networks and biomicrometeorological research. Previous studies have hypothesized potential underestimation of the vertical velocity turbulent perturbations, necessitating correction to increase flux measurements by approximately 10%, while some studies have refuted that any correction is needed. Those studies have used cross comparisons between sonic anemometers and numerical simulations. Here we propose a method that yields a correction factor for vertical velocity that requires only a single sonic anemometer in situ but requires some assumptions and adequate fetch at a sufficient distance above roughness elements where surface similarity is valid. Correction factors could be important in adjusting flux network and other flux data, as well as assessing the energy budget closure that is used as one of the flux data quality measures. The correction factor is confirmed in one field experiment and comparison between a CSAT3 and RMY 81000VRE, but it does not work well for the more complex form factors shown in a field comparison of an IRGAson and a CSAT3a.

1 Introduction

Three-axis sonic anemometers logged at high frequencies (usually 5 Hz to 60 Hz+) are in widespread use in trace gas exchange, energy budget, and micrometeorological studies. These devices, like virtually all instrumentation, have some limitations and may need corrections and calibration. The most prevalent 3-axis sonic anemometers use non-orthogonal axes, with the firmware calculating high frequency orthogonal axes velocity components, the sonic temperature (approximately the virtual temperature), or the wind vector direction and magnitude. Compared with sonic anemometers with orthogonal axes where transducer pairs are located 90 degrees from each other, non-orthogonal sonic anemometers transducers are clustered with angles less than 90 degrees. In non-orthogonal sensors, flows from each velocity component are not independent, so post-processing corrections within the anemometer firmware are performed to separate individual orthogonal velocity components. Because non-orthogonal sonic anemometers are used in multiple sites around the world, such as in international networks like FLUXNET and AmeriFlux, to calculate quasi-continuous carbon dioxide and water exchange, and the energy budget including sensible heat, any correction to their measurements is very important. In the past decade, extensive discussions have arisen on whether non-orthogonal flux measurements need correction for potential flow distortion, and if so, how large the correction should be. This discussion is very important to decreasing potential bias errors in trace gas exchange measurements such as carbon and water vapor fluxes, in addition to helping balance energy budget closure.

Studies about potential correction factors have involved 1) comparing non-orthogonal sonic anemometers with orthogonal designs; 2) orienting and comparing sonic anemometers, including at different vertical angles both in the field and in wind tunnels; 3) numerical and analytical fluid dynamic simulations of flow around the anemometer configurations and idealized shapes; or 4) examining the spectral output of the anemometers (Wyngaard 1981; Mortensen and Hojstrup 1995; Foken et al. 1997; Beyrich et al. 2002; Loescher et al. 2005; Nakai et al. 2006; Mauder et al. 2007; 2013; 2018; Kochendorfer et al. 2012; Frank et al. 2013, 2016, 2020; Horst et al. 2015, 2016; Huq et al. 2017; Pena et al. 2019). While many of these studies have noted underreporting of the turbulent vertical velocity fluctuations by more than 10% in for some anemometer types, others have found little correction is needed for the vertical velocity (as shown in Table 1).

Table 1. Summary of some selected previous research on vertical velocity correction factors

Anemometer Type	Vertical Flux (velocity) Correction Factor	Paper/Author	Notes
Campbell Scientific CSAT3	3-5%	Horst et al. 2015	Wind Tunnel tests, field comparison with orthogonal design
Campbell Scientific CSAT3	3-7%	Huq et al. 2017	Numerical Flow Simulation including oscillating velocities
Campbell Scientific CSAT3	8-10%	Frank et al. 2013, 2016	Field comparison including orthogonal design
Campbell Scientific CSAT3	14%	Kochendorfer et al. 2012	Field comparison including orthogonal design
Campbell Scientific CSAT3	0%	Loescher et al. 2005	Wind Tunnel, Field Comparison including orthogonal design
Campbell Scientific CSAT3	~~10~~5-12%	Mauder et al. 2007	Field comparison including orthogonal design; authors used CSAT3 as standard, correction factor here assumed orthogonal designs should be considered the standards
Campbell Scientific CSAT3	2-3%	Mauder 2013, Mauder and Zeeman 2018	Field comparison including orthogonal design
Metek uSonic-3	22-32%*	Horst et al. 2015	*Maximum correction at high vertical angles and expressed along the sonic path direction converted to vertical velocity, this maximum would be around 70% of the value at an extreme flow vertical angle of 45° ; overall correction factor not presented but expected to be somewhat lower; Wind tunnel study
Metek uSonic-3	3%	Mauder and Zeeman 2017	Field comparison against Gill-HS as a standard
Metek USA-1~~Metek USA-1~~	<1% corrected; 33%~~<5% uncorrected~~	Pena et al. 2019~~Beyrich et al. 2002~~	Spectral analysis in the inertial subrange
RM Young 81000VRE~~Metek USA-1~~	10-15% (12%) ~~33%~~	Kochendorfer et al. 2012~~Pena et al. 2019~~	Field comparison including orthogonal design
RM Young 81000VRE~~RM Young 81000VRE~~	-2 % ~~10-15% (12%)~~	Mauder and Zeeman 2018~~Kochendorfer et al. 2012~~	Field comparison against Gill-HS as a standard
RMYoung 81000~~RM Young 81000VRE~~	22%**~~-2 %~~	Foken 1999~~Mauder and Zeeman 2018~~	** Field comparison with CSAT3
Campbell Scientific IRGason~~RMYoung 81000~~	2-9%***~~22%*~~	Polonik et a. 2019~~Foken 1999~~	***Field comparison with Gill R2~~*Compared to CSAT3~~
Campbell Scientific IRGason~~Campbell Scientific IRGAson~~	<0.5% - 4%~~5-9%**~~	Horst et al. 2016~~Polonik et a. 2019~~	Wind tunnel and field comparison to CSAT3~~**Compared to Gill R2~~
Solent Gill HS-50~~Campbell Scientific IRGAson~~	0% (assumed as standard); 0% compared to CSAT3~~<0.5%~~	Mauder et al. 2017; Mauder & Zeeman 2018~~Horst et al. 2016~~	Field comparison at 3 m height, 25 cm grass canopy

Solent Gill HS-50/HS-100~~Solent Gill HS-50~~	-10-+15%~~0% (assumed as standard); 0% compared to CSAT3~~	Glabeke et al. 2024~~Mauder et al. 2017; Mauder & Zeeman 2018~~	Wind tunnel study HS-100 has same form factor as HS-50~~3 m height, 25 cm grass canopy~~
Solent Gill R3-50~~Solent Gill HS-50/HS-100~~	13-35%~~-10-+15%~~	Frank et al. 2020~~Glabeke et al. 2024~~	Field comparison including orthogonal design~~Wind tunnel study~~ ~~HS-100 has same form factor as HS-50~~
Solent Gill R3-50~~Solent Gill R3-50~~	5-13%~~13-35%~~	Nakai et al. 2006~~Frank et al. 2020~~	Angle of attack analysis for measurements over 2 forests and a bog
Solent Gill R2~~Solent Gill R3-50~~	7%~~5-13%~~	Mortensen & Hojstrup 1995~~Nakai et al. 2006~~	Lab and wind tunnel analysis
~~Solent Gill R2~~	~~7%~~	~~Mortensen & Hojstrup 1995~~	

In this paper, we test a method that involves standard turbulence data from any individual sonic anemometer (the standard deviation of the vertical velocity, σ_w, and the friction velocity, u*). From the rtio σ_w /u* from any single sonic anemometer under near-neutral conditions, a vertical velocity correction factor can be determined, which can henceforth be applied to vertical flux exchange measurements. Although previous papers have discussed using σ_w/u* to test correction factors derived independently by other fashions and/or a qualitative assessment of measurement validity (Horst et al., 2015, Lloyd 2023, Wang et al. 2016), none, that we have found, suggest using that ratio itself can independently determine the correction factor. Multiple sonic anemometers do not have to be used for cross-comparison, and some assumptions or limitations used in computational flow simulations at lower Reynolds numbers and wind tunnel studies that have different turbulence regimes, all not necessarily representing field conditions, are not needed. However, our method, as tested here, is not able to examine the change in correction factors with stability as in Horst et al. (2015), but, if an assumed σ_w/u* relationship is known independently as a function of stability, the method could be extended to non-neutral conditions. We test our method on four types of non-orthogonal anemometers (CSAT-3/CSAT3a, IRGAson, Solent Gill HS-50, and RM Young 81000VRE "Long-Neck"), used in seven independent field campaigns, spanning over a decade in time and in two continents, and directly compare the results of the correction factors by comparing the vertical flux calculations from CSAT3 and RM Young 81000VRE bare ground field data, and from CSAT3a and IRGAson bare ground field data, under a wide range of stabilities. We use bare ground or short stubbled surfaces primarily to develop the method under relatively ideal conditions.

2 Methodology

2.1 Theory

Our method is based on previously derived sonic data (generally orthogonal sensor design with a vertical sensor path orientation, except Thurtell et al.,1970 which was a pressure sphere anemometer) showing near-neutral ratio of σ_{wm}/u* is constant at around 1.3, or, to two significant figures, 1.25 (Thurtell et al. 1970; Haugen et al. 1971; Wyngaard et al. 1971; Merry and Panofsky, 1976; Panofsky et al. 1977; Panofsky and Dutton, 1984; Sharan et al. 1999). The original Kansas experiment data used Kaijo-Denki PAT-311 sonic anemometers (Haugen et al. 1971) with a vertical probe path, orthogonal to the plane of the horizontal axis paths. Given that the vertical velocity could be affected by sensor configuration and flow distortion, we define a factor (C_w) that corrects for the potential underestimation of measured vertical velocity w_m (Eq. 1). We assume that any given sonic anemometer should give this ratio under near-neutral conditions. If a sonic anemometer reports a ratio that is lower than 1.25, we can use C_w such that the corrected ratio is 1.25. We recognize that orthogonal sonic anemometer designs may also exhibit flow distortion in the x and y directions, while less likely to distort flow in the vertical direction. This is discussed briefly below further. We also note that if the true σ_w/u* value were to be assumed equal to 1.2 or 1.3 instead of 1.25, the correction factors we report would need adjustment to be approximately 8% lower or 8% higher, respectively.

Applied to non-orthogonal sonic anemometers, the factor C_w can be multiplied by the measured σ_{wm} to correct for vertical velocity underestimation (Eq. 1). Below we use the subscript "m" to indicate sonic anemometer measured values. On the other hand, for correcting measured u*, the factor would translate to the square root of C_w, because u* is the square root of $\overline{u_m w_m}$ (or even if $\overline{v_m w_m}$ is used in defining u*, the same result would occur). As shown in the equations (2 and 3), the near-neutral ratio of 1.25 to the measured σ_{wm} over measured u* (below assuming negligible $\overline{v_m w_m}$ contribution) reported by a sonic anemometer yields the square root of C_w, allowing one to solve for C_w.

$$w = C_w w_m;\ \sigma_w = C_w \sigma_{wm} \tag{1}$$

$$\overline{uw} = C_w \overline{w_m u};\ u^* = \sqrt{C_w \overline{uw_m}} = \sqrt{C_w} u_m^* \tag{2}$$

$$\frac{\sigma_w}{u^*} = \frac{C_w \sigma_{wm}}{\sqrt{C_w} u_m^*} = \sqrt{C_w}\frac{\sigma_{wm}}{u_m^*} = 1.25 \tag{3}$$

$$\sqrt{C_w} = \frac{1.25}{\frac{\sigma_{wm}}{u_m^*}} \tag{4}$$

$$C_w = \left(\frac{1.25}{\frac{\sigma_{wm}}{u^*_m}} \right)^2 \quad (5)$$

We assume that for non-orthogonal anemometers, the horizontal velocities u and v are not significantly underestimated because the typical sensor and physical structure are generally relatively open in the horizontal plane. However if they are affected either by the physical structure or firmware used to calculate orthogonal components or both, the following correction factors for the longitudinal velocity (C_u) and cross-wind velocity (C_v) could be put into the equation (2) for the more comprehensive equation of u*, especially above the surface layer, in the boundary layer where $\overline{v_m w_m}$ may be appreciable:

$$u^* = \sqrt[4]{C_u^2 C_w^2 (\overline{u_m w_m})^2 + C_v^2 C_w^2 (\overline{v_m w_m})^2} = \sqrt{C_w} \sqrt[4]{C_u^2 (\overline{u_m w_m})^2 + C_v^2 (\overline{v_m w_m})^2} \quad (6)$$

Equation 6, if C_u and C_v both equal one under ideal conditions, collapses to equation 2 for the u* correction, where u* could be either based on the surface layer $\overline{u_m w_m}$ or the basic equation expanded in equation 6 for conditions when $\overline{v_m w_m}$ cannot be ignored. It should be noted that some surface layer sonic anemometer rotation protocols include the "roll" rotation where $\overline{v_m w_m}$ is minimized, whereas the first two rotations are more straightforward and are more commonly used, for pitch and azimuthal (yaw) axis rotations. The same considerations could be applied to orthogonal sonic anemometers, that is, their horizontal velocity components could be distorted (Frank et al. 2016) as earlier alluded to. This has the implications that equation 6 could still be used in this case, but the value of 1.25 in the earlier equations might require modification, if the horizontal component distortion effects influenced the friction velocity u*.

Because we are considering only near-neutral conditions, we do not have to worry about the correction factor iteratively influencing the stability parameter (z/L), as z/L will be close to zero anyway. The method can also be used to examine if the correction factor is dependent on azimuthal angle, so long as near neutral conditions occur at those angles. We note our assumptions might not always be strictly applicable, with the non-orthogonal physical configurations coupled with different firmware versions pushing the limits of our assumptions. Also, we assume that the correction factor would be approximately the same in near-neutral conditions as in non-neutral conditions, which

may not be true based on the potential for increased pitch angles in turbulent eddies, changing the shadowing factors of sonic anemometer design.

By plotting σ_w/u^* versus z/L, we determined the limits of near-neutrality conditions by observing a zone where σ_w/u^* was approximately constant. In most cases, this was in the z/L range between -0.10 and 0. Our data showed a slight increase in σ_w/u^* as the stability transitioned from near zero to stable conditions with $z/L > 0$, so we limited near neutral stability conditions to the slightly unstable values of z/L. In our datasets, the $\overline{v_m w_m}$ contribution to u* was generally negligible compared to $\overline{u_m w_m}$, because we were measuring in the surface layer, so equation (2) could be used.

2.2 Experimental Setup & Data Used

The field campaigns examined here involved bare ground or short stubble with over 100:1 fetch-height ratios. Sonic anemometer data were rotated into the mean wind (azimuth rotation) and vertically (pitch rotation) and were not subject to planar rotation as described by Paw U et al. (2000). Data from a total of 13 Campbell Scientific Incorporated (CSI CSAT3's) were used, of which 12 were used to yield uncertainty estimates for the correction factor. The CSAT3's were examined in four independent field campaigns, with most of the CSAT3 20 Hz data taken from five CSAT3's at 3.45 m height and five CSAT3's at 6.90 m height, and summarized in ½ hour periods, from the HATS experiment (Kleissl 2003). Two CSAT3's were used at the University of California Davis Campbell Tract experimental site (38° 32.2' N, 121° 46.7' W, 18 m asl) during two different field campaigns, with one CSAT3 at 0.93 m in 2011, and the other in 2005 at 1.2 m (Kochendorfer and Paw U 2011) and another CSAT3 in a 2018 UC Davis Delta evapotranspiration project (Paw U et al. 2019) at 1.5 m, with data gathered at 10 Hz and summarized for ½ hour periods. One CSAT3 was used in an independent comparison with an RMYoung 81000 at the C10 site in Roberts Island of the Delta region of the Sacramento-San Joaquin Valley in a UC Davis Delta project (Paw U et al. 2019).

One CSAT3a was studied in a comparison with an IRGAson in the Delta site 113, Courtland, California, USA (38°18'58.59" N, 121°32'49.24"W, 4 m asl). Both sensors were installed at 1.7 m from the soil surface, faced the same direction, and were separated horizontally by a 3.2 m distance. For both sonics, data was gathered at 10 Hz and processed using EddyPro., without the shadow correction option selected (see below for a rationale in the discussion of the Horst et al. 2015 results). Two additional IRGAson's were also studied without another sonic anemometer present for comparisons. One IRGAson[2] was installed in Clarksburg, California, USA (38°21'47.16"N,

121°34’10.85”W, 3 m asl) at a height of 1.25 m (Delta site 55), while the other was deployed at Walnut Grove, California, USA (38°15’5.55”N, 121°35’3.18”W, 3 m asl) at a height of 1.8 m (Delta site 34). For the IRGAsons, data was gathered at 10 Hz and processed using EddyPro. For the RM Young 81000VRE anemometers, the UC Davis Delta evapotranspiration project campaign data were used for the sonic anemometers mounted at 1.5 m at two different field sites, Roberts Island and Union Island (Paw U et al. 2019), with data logged at 5 Hz. Note that because the RM Youngs are internally sampling data at 160 Hz, the 5 Hz logging rate does not result in any frequency related covariance underestimation but can have a slightly greater statistical uncertainty (Bosveld and Beljaars 2001, Paw U et al. 2018). For the Solent Gill HS-50 sonic anemometers mounted at 2 m, 10 Hz data were from the LIAISE experiment in Spain. The anemometers were mounted on arms oriented 180^{o} from each other. The Land surface Interactions with the Atmosphere in the Iberian Semi-Arid Environment (LIAISE) field experiment took place in the Lleida Region of Catalunya, Spain in the spring and summer of 2021. Although the purpose of the LIASE experiment was to study the impact of agriculture on the water cycle in irrigated regions, there were extensive surface energy budget, surface layer, and boundary layer measurements. One of the LIAISE sites, Els Plans, was located at a fallowed winter wheat field. There was remaining hay and stubble on the ground, so it was not completely bare soil. A 50 m mast was installed at Els Plans which included eight Gill HS-50s mounted at 2, 10, 25 and 50 m AGL (Brooke et al., 2024). In this study, we use only the 2 m height to ensure that measurements are in the surface layer. There were two anemometers located at 2 m height: “Sonic A” with an orientation of 338° and “Sonic B” with an orientation of 158°.

Table 2. Summary of Field Experiments used in this Study

Field Experiment	Sonic Type & Number	Height	Dates	References
HATS	10 x CSAT3	3.45 m & 6.90 m	9/2/2000-9/9/2000	Kleissl et al. 2003
UCD Campbell Tract	1 x CSAT3	0.93 m	7/29/2011-11/22/2011	Kochendorfer and Paw U, 2011
UCD Campbell Tract	1 x CSAT3	1.2 m	8/16/2005-9/6/2005	
Delta Roberts Island	1 x CSAT3	1.5 m	8/15/2018-9/16/2018	Paw U et al. 2019
Delta Roberts Island & Union Island	2 x RM Young 81000	1.5 m	7/10/2018-10/10/2018 8/24/2018-11/7/2018	Paw U et al. 2019
LIAISE	2 x Gill HS-50	2 m	7/15/2021-7/30/2021	Boone et al. TBD Mangan et al., 2023
Delta sites 34, 55 (Walnut Grove, Clarksburg)	2 x IRGAson	1.5 m	9/13/2023-10/19/2023	

Delta Site 113 (Courtland)	1 x IRGAson, 1 x CSAT3a	1.5 m	6/13/2024-7/2/2024	

σ_w/u* data were filtered for wind directions coming into the anemometer in a default range of +/-45 degrees centered towards the maximum fetch and sonic anemometer orientation, in the opposite direction from the tower/mast mounts, to minimize the influence of any flow distortion not caused by the transducers and their mounts. Different ranges of azimuthal angles were examined. For the 10 HATS CSAT3's that had two heights, 3.45 m and 6.90 m, with 5 individual CSAT3's at each height, data were used only when approximately constant flux conditions existed, that is, when the u* between the two heights were within 5% of each other. Near neutral was defined as unstable conditions with zeta >-0.1 and < 0.00 for most cases, except for the RM Young 81000VRE case where the near neutral constant zeta was observed for zeta > -0.1~~05~~ and zeta < 0.0~~40~~ (see Fig. 1). Zeta is defined here as z/L, where z is the height of measurement, and L is Monin-Obukhov length.

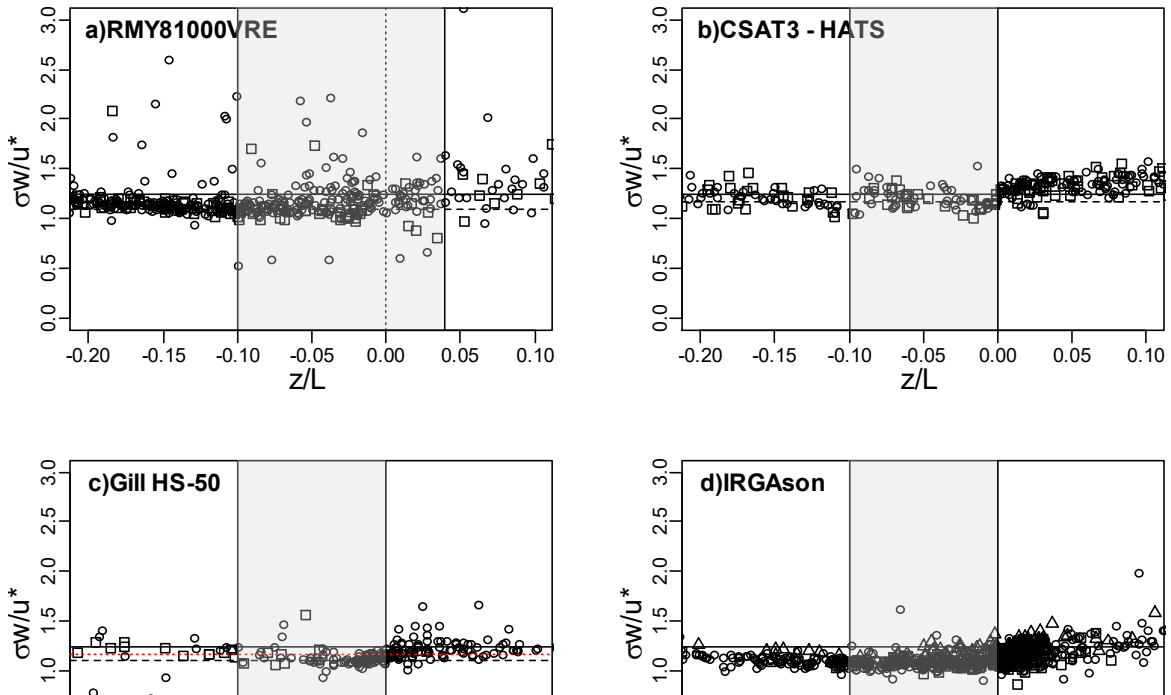

Figure 1: Vertical standard deviation ratio divided by friction velocity (σ_w/u^*), as a function of stability z/L in the near-neutral interval of -0.20 to 0.10, for four sonic anemometer types. Vertical lines show near neutral ranges used to determine C_w. A horizontal line indicates the assumed 1.25 ratio. a) Upper left, for the RMY 81000VRE, b) upper right, for the HATS CSAT3's, c) lower left, Gill HS-50 sonic anemometer, d) lower right, IRGAson sonic anemometers, circles for site 113, squares for site 55, and triangles for site 34. Dashed lines indicate the median ratio (σ_w/u^*) determined in the near-neutral range; for the Gill HS-50, the long black dashed lines indicate the median ratio for "Sonic B" and the shorter red dashed lines indicate the median ratio for "Sonic A."

At the UC Davis Delta Roberts Island C10 site, both an RM Young 81000 and a CSAT3 were run at the same time, so an applications test of our theory was made by correcting both the CSAT3 and the RM Young 81000 sensible heat H data with their respective C_w correction factors to see if the corrected data from the two separate sonic anemometers would agree better than if they were uncorrected. At the Delta Site 113-, a test of the theory was made by comparing a CSAT3a with an IRGAson, to see if the theoretical correction factors matched the sensible heat H data for these two sonic types.

3 Results and Discussion

3.1 Correction Factors C_w

This method yields vertical velocity and vertical flux C_w correction factors compatible with previous studies using other methods, especially for the CSAT3's. Of the four sonic anemometer types analyzed, the IRGAson (see further discussion below) and RMYoung "long neck" anemometers had the greatest C_w correction factors of 1.1923-1.37, and

the Solent Gill HS-50's, 1.21 (average of 1.283 and 1.137), the CSAT3's, and the CSAT3a had correction factors of 1.11-1.23 (median 1.13), with a standard deviation of 0.07 for the 13 CSAT3 anemometers.

Table 3. Vertical Velocity Correction Factors C_w Calculated in this Study

Field Experiment	Sonic Type & Number	Correction Factor C_w	Standard Deviation C_w	Number of Sonics
HATS	10 x CSAT3	1.13	See below	10
UCD Campbell Tract	1 x CSAT3	1.12	See below	1
UCD Campbell Tract	1 x CSAT3	1.23	See below	1
Aggregate	13 x CSAT3	1.13	0.069	12
Delta Roberts Island (C10)	1 x CSAT3 1 x RM Young 81000	Used only for independent cross comparison	--	2
Delta Union Island and Roberts Island	2 x RM Young 81000	1.283	0.13	2
LIAISE	1 x Gill HS-50	1.21	0.1	21
Delta sites 34, 55 (Walnut Grove, Clarksburg)	2 x IRGAson	1.37*	*	2
Delta site 113 (Courtland)	1 x IRGAson	1.33*	--	1
Delta site 113 (Courtland)	1 x CSAT3a	1.11	--	1

*Cross comparison with CSAT3a indicates assumptions made to calculate the theoretical C_w are not fully applicable for the IRGAson form factor. The IRGAson practical correction factor C_w should be the same as the CSAT3a, as explained in the text.

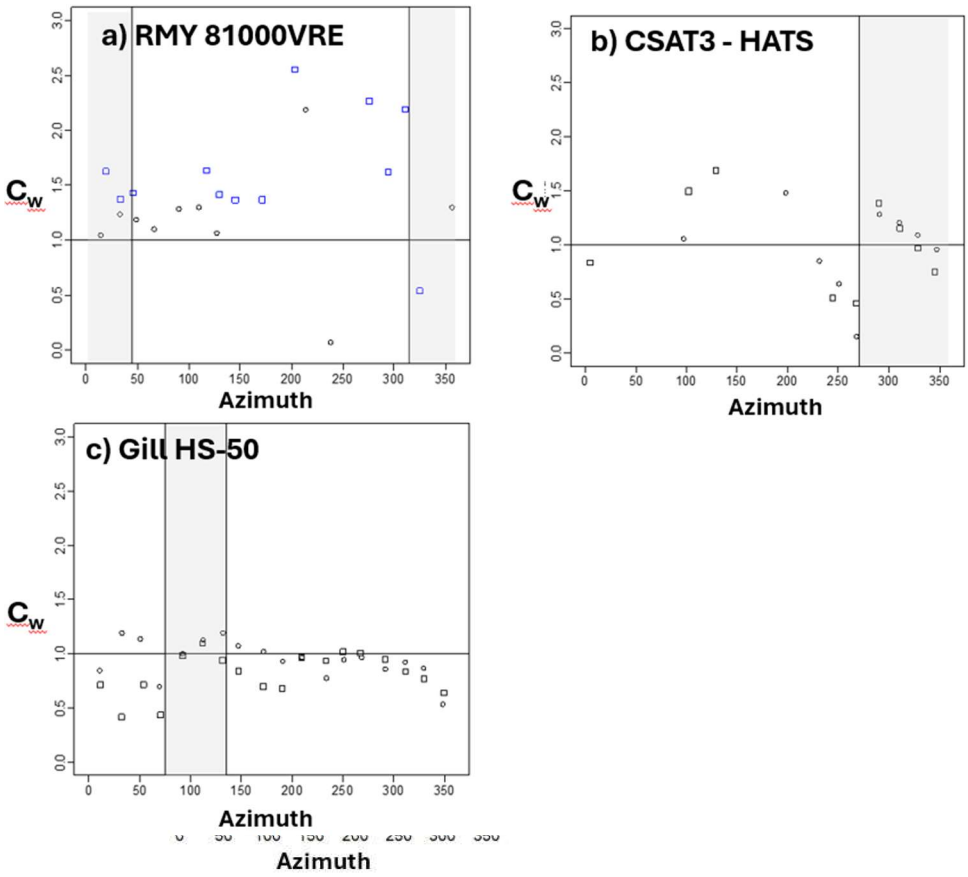

Figure 2: Correction factor C_w for a) the RM Young 81000VRE's as a function of azimuthal angle relative to North (upper left), HATS CSAT3's (upper right), and the Gill HS-50's (lower left). The vertical lines and gray shading represent the optimum angles between 315º and 45º as assessed during the experimental design phase (upper left), 270º and 360º (upper right), and between 97 º -187º for the circles, and 277 º -7º for the square symbols (lower left)~~270º and 360º (upper right), and 60º and 150º (lower left)~~. For the RM Young 81000's, the circles represent data from the Roberts Island site, and the squares, Union Island. For the CSAT3's, the circles represent the median for 5 sonic anemometers at the 3.45 m height and the squares, 5 sonic anemometers at the 6.90 m height. For the Gill HS-50, the circles represent a sonic on the arm oriented to the East, and the squares, the sonic on an arm oriented to the West, with block medians taken for the correction factors spanning 20º intervals.

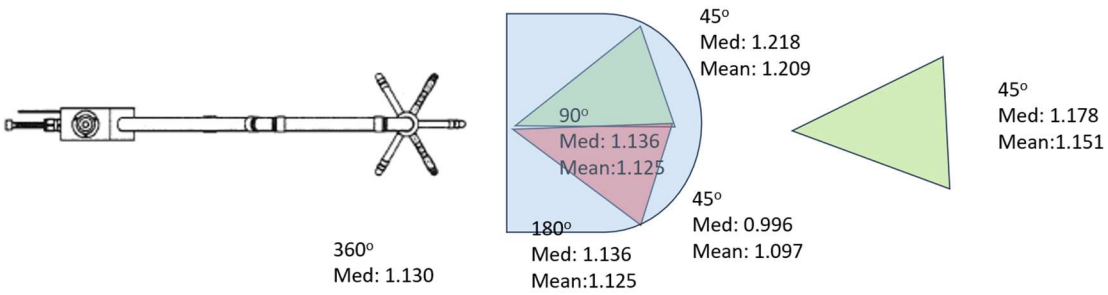

Figure 3: Correction factor C_w as a function of azimuthal angle sectors, for the HATSs CSAT3 data.

The proposed method was tested for correction factor C_w as a function of azimuthal angle ranges for the Gill HS-50's (Fig. 2). The proposed method was also tested for correction factor C_w as a function of azimuthal angle ranges for the CSAT3's (Figs. 2 & 3). Because the IRGAson geometry is asymmetrical when viewed in the x-axis direction of the sensor, we examined correction factors for different azimuthal angles. However, the details of the IRGAson are not presented here, as we present evidence that our theoretical method's assumptions appear not to have been met when analyzing the IRGAson.

3.2 Sonic Anemometer Field Intercomparisons

The correction factors were tested on the CSAT3 and RM Young 81000 sited in the Delta fallow field for the sensible heat. When the CSAT3 was corrected with the average CSAT3 factor of 1.13, while the RM Young 81000 corrected by it's individual correction factor using our method (1.188), there was excellent agreement (Fig. 4, slope of 0.9947, intercept of -0.538 W m^{-2}) but when the RM Young 81000 was corrected by the average factor from Table 4 (1.28), the sensible heat of the RM Young 81000 was overcompensated (slope of 1.07, intercept of -0.58 W m^{-2}) (not shown in Figures). The uncorrected sensible heats showed the RM Young 81000 H was lower than that for the CSAT3 (slope of 0.947, intercept of -0.453 W m^{-2}, Fig. 4).~~The correction factor tests on the CSAT3 and RM Young 81000, carried out on the Delta fallow field for the sensible heat yielded good agreement (slope of 1.024, intercept of -0.06 W m^{-2}) after the corrections were applied to both anemometers, in contrast to the uncorrected data (slope of 0.953, intercept of -2.58 W m^{-2}, Fig. 4)~~. The excellent agreement implies the correction method is applicable for a range of stabilities, and not confined to near-neutral conditions, for vertical scalar fluxes, for these two sensor head configurations but that some uncertainty in correction can occur when using the average correction factors.~~.~~ The uncorrected vertical velocity standard deviation shows the RM Young 81000 was lower than the CSAT3 (slope of 0.9035,intercept of 0.000511 m

s^{-1}), while the corrected data had a slope of 1.0235 and an intercept of 0.000654 m s^{-1} (Fig. 4). The agreement for u*, on the other hand, was not as good, although it still improved the agreement, with a corrected (for the individual RM Young 81000) slope of 0.9384 and intercept of 0.032 m s^{-1}~~slope of 0.877 and intercept of 0.047 m s^{-1}~~, compared to the uncorrected slope of 0.8817 ~~0.842~~ with an intercept of 0.0285~~0.043~~ m s^{-1} (Fig. 5). The figure shows a great deal of overestimated scatter for the RM Young u* in the intermediate range of u* from around 0.05 m s^{-1} to around 0.2 m s^{-1}; taking block medians of the data over intervals of the x axis, to reduce the effect of the scatter did not change ~~improved~~ the regression ~~slightly~~results much, ~~the slope improving to~~a similar slope of 0.934522 and intercept at 0.0301~~1~~ m s^{-1} (Fig. 5). This implies some of the assumptions we have made may be violated in terms of the distortion or firmware influences on the horizontal velocity measurements and the correlation coefficient between the vertical and horizontal velocity components, when applied to a range of stabilities. This issue affects the u* calculation more than the simpler vertical velocity correction for the scalar sensible heat flux.

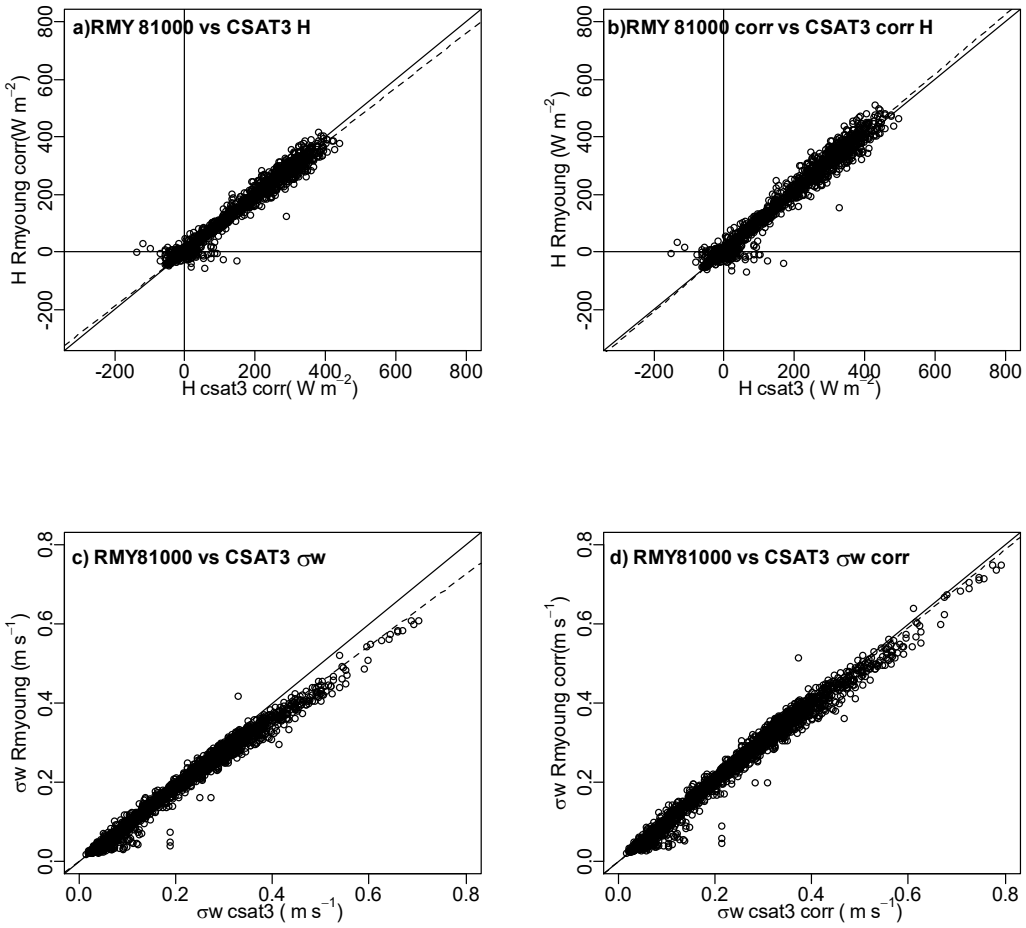

Figure 4: a) Uncorrected RMYoung 81000VRE sensible heat plotted against uncorrected CSAT3 sensible heat, with regression line Y=0.9465X – 0.4533 W m^{-2} shown by a dashed line and 1:1 line shown by a solid line b) Corrected RMYoung 81000VRE sensible heat plotted against corrected CSAT3 sensible heat, with regression line Y= 0.9947X – 0.5383 W m^{-2} ~~1.0302X – 0.5575~~ shown by dashed line. c) Uncorrected RMYoung 81000VRE σ_w plotted against uncorrected CSAT3 σ_w with regression line Y = 0.90354X + 0.0005112 m s^{-1} shown by dashed line. d) Corrected RMYoung 81000VRE σ_w plotted against corrected CSAT3 σ_w with regression line Y = 1.0235X + 0.0006543 m s^{-1} ~~0.98350X + 0.0006287~~ shown by dashed line.

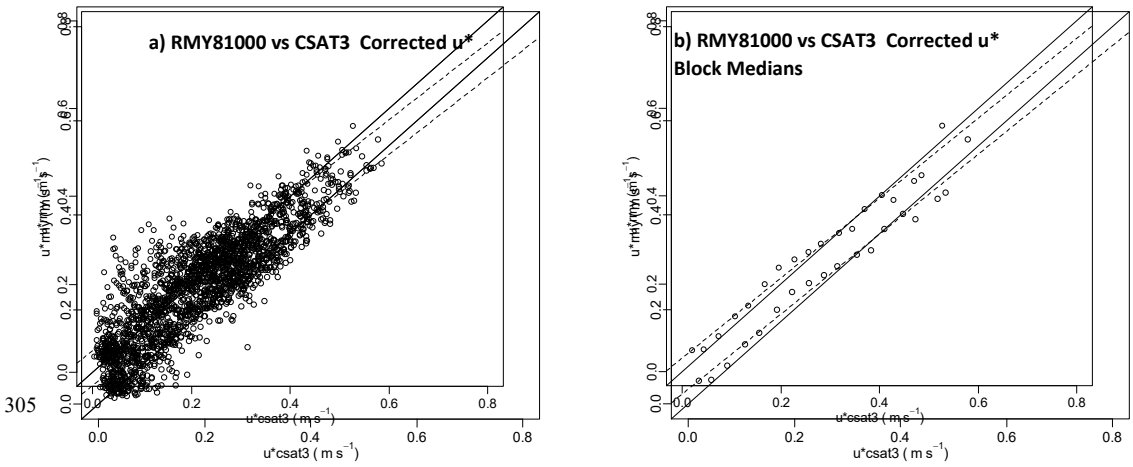

Figure 5: a) Corrected RMYoung u* plotted against corrected CSAT3 u*, Y=0.9384X – 0.03225 m s^{-1} b) Block ~~. Y=0.8771X – 0.0472~~ b) Block medians of corrected RMYoung 81000 u* plotted against corrected CSAT3 u*, Y=0.9345X +0.0302 m s^{-1} ~~. Y=0.9138X +0.0285~~.

In the field test between the CSAT3a and the IRGAson, sensible heat covariance $\overline{w'T'}$ was within 1%, and the σ_w was also within 1% (Fig. 6). This implies the vertical velocity correction factor for the IRGAson should be considered the same as for the CSAT3a, that is a C_w of around 1.11, similar to that for CSAT3's. However, our analysis method results in a C_w of 1.33-1.37 for the IRGAson (Table 3), which is in contrast to the direct comparison between the two anemometers. Analysis of the data shows the IRGAson u* was greater than that for the CSAT3a, including during

315 near-neutral conditions, creating a greater value for C_w (Fig. 6). This was not seen in the standard deviations of the longitudinal and vertical wind components but did show up in the cross-wind standard deviation (matching earlier reports of the cross-wind anomalies in Horst et al. 2016), so this implies that either the complex sensor head geometry, the internal data processing, or both yielded this overestimate of Reynolds stress covariance and u* while not relatively affecting the vertical velocity measurements compared to the CSAT3a (Fig. 6). Horst et al. (2016) reported that the
320 IRGAson yielded a lower u* than their reference CSAT3's, but they calculated their u* as the surface layer stress based on $\overline{u'w'}$ while we were using the total Reynolds stress term with both $\overline{u'w'}$and $\overline{v'w'}$, which could explain our different results for u*. The basic assumptions in our theory, that only the vertical velocity would be affected, and that that effect would propagate into u* as a square root relationship compared to a direct propagation into the vertical velocity, were apparently not appropriate for the IRGAson. This result also means that using the departure of the
325 IRGAson's ratio σ_w/u* from the idealized 1.25 value cannot be used as a general quality control assessment for its vertical eddy covariance measurements, a method suggested in some sources (Horst et al. 2016; Wang et al. 2017; Lloyd 2025).

330

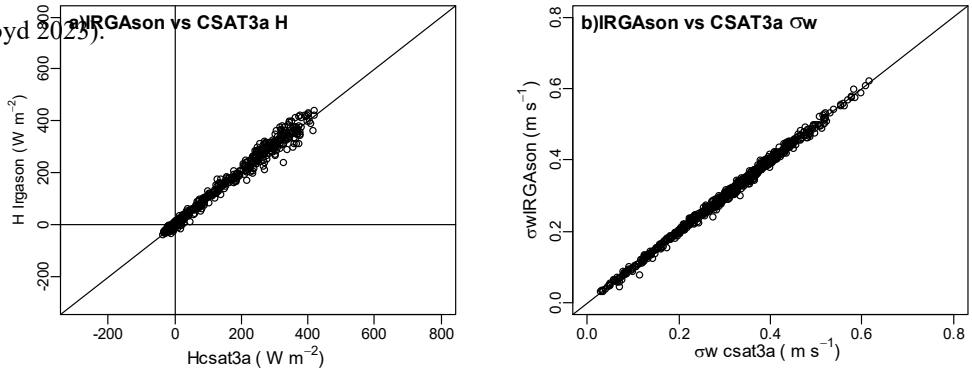

335

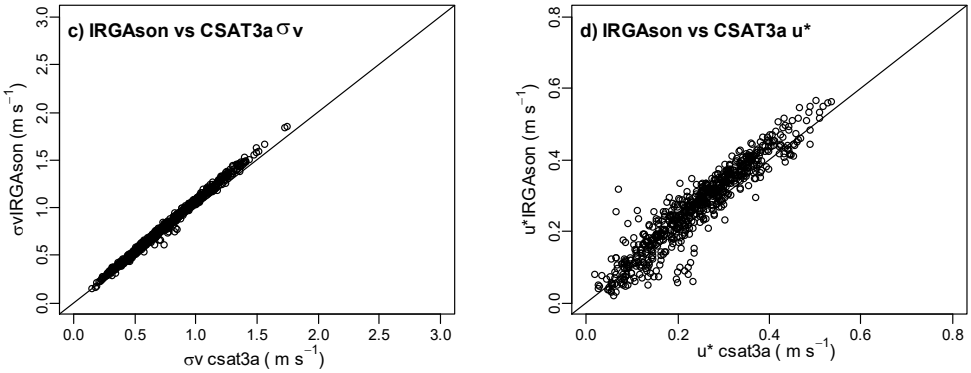

Figure 6: Comparison of a) Sensible Heat, H, b) vertical velocity standard deviation, σ_w, c) cross wind velocity standard deviation σ_v and d) u* between the CSAT3a and IRGAson at Delta site 113.

Literature data for the ratio of σ_w/u^* in near-neutral conditions also were generally compatible with our analysis. While the CSAT3/CSAT3a C_w correction factors (1.11-1.23, median 1.12) are close to literature CSAT3 values (1.03-1.14) the literature IRGAson factors of 1.005-1.09 are somewhat lower than our theory's calculation of 1.33-1.37, but similar to the correction factor of 1.11 for the IRGAson when based on the theoretical correction factor for the CSAT3a and the observed equivalence of the sensible heat and vertical velocities between these two sonic head configurations at a common test site. Horst et al. (2015) reported a σ_{wm}/u^* value of 1.17 for uncorrected CSAT3 data, which using our method would yield a C_w of 1.14, well within our range of CSAT3 C_w results. They also reported a similar σ_{wm}/u^* value (1.16) for the shadow correction that can be implemented in models like the CSAT3a or IRGAson, so it appears that implementing the built-in shadow correction option would not affect our method or results. Interestingly, the method applied to instruments over tall canopies yields comparable values to the literature and our study, but with some difference. Wang et al. (2016) report for a 10 m forest canopy and sonic anemometers 5 m above this height, the near neutral σ_w/u^* values of 1.19 and 1.18 for and IRGAson and Gill Windmaster, which would translate to C_w correction factors of 1.10 and 1.12 respectively using our method. The RM Young 81000 comparison by Foken (1999) of a 22% correction relative to a CSAT3 would translate to an absolute correction of 38%, or higher than our value of 28~~3~~%, if the CSAT3 is considered to have a 13% correction. The Gill HS-50 results of 21% correction is higher than the range of literature values. The lowest literature value was assumed to be 0% (Mauder et al. 2017), and approximately equal to the CSAT3 when compared with other sonic anemometers (Horst et al. 2016); which would then imply a 13% correction, to from between -10% to +15% (Glabeke et al. 2024).

4 Summary and conclusions

We present a method to estimate vertical velocity and flux corrections for sonic anemometers, using turbulent statistics from a single anemometer, instead of comparisons that require the test anemometer and reference orthogonal sonic anemometers to be side by side, laboratory or numerical methods, or methods requiring raw high frequency data. The vertical velocity factor C_w is multiplied by vertical eddy covariance fluxes to correct them for transducer shadowing. This method could provide correction factors associated with objects near the test anemometer, such as the tower or

mast mounting assembly, electronic support environmental enclosures, solar panels, etc., in addition to transducer and sonic anemometer head design flow distortion to the vertical wind speed.

Application of our correction method could improve energy budget closure by 10% to over 20% depending on the anemometer type, and would thereby increase calculated eddy-covariance based fluxes. Several assumptions are made which may not always be applicable, and here we present tests over relatively ideal sites with low roughness (bare ground and good fetch). Our study demonstrates the standard deviation of the vertical velocity and friction velocity data gathered under near-neutral stability from an individual sonic anemometer can be used to estimate a vertical velocity and vertical flux correction factor, for some of the most common sonic anemometers, under any stability conditions. The values are consistent with literature for the CSAT3 range of suggested correction factors (1.13), the CSAT3a at 1.11, and the Gill HS-50 (1.21), while the correction factors for the RM Young VRE is higher, 1.283. The theoretical correction factor of 1.33-1.37 for the IRGAson did not match results from a direct comparison with a CSAT3a, and implied the CSAT3a correction factor of 1.11 should also be used for IRGAson's. This implies our theory's assumptions did not appear valid for the IRGAson configuration, partially because of cross-wind turbulence overestimation probably related to the relatively complex IRGAson form factor. Our results also mean that one general quality assessment of eddy-covariance vertical fluxes, based on the closeness of the near-neutral values of σ_w/u^* to 1.25, cannot be reliably applied to the IRGAson or other similar sonic anemometer systems with unusual shape/form factors, but is appropriate for usage with typical sonic anemometers like the CSAT3 family, RM Young 81000VRE the Gill HS-50, and similar anemometers. This form of analysis could be tested in the future for usage over taller roughness landscapes, such as crops, orchards and forests, given enough fetch for measurement heights over the roughness layer.

Code and Data Availability

Data are available upon request from the authors Kyaw Tha Paw U and Mary Rose Mangan.

Author Contributions

KTPU and MRM designed the study with input from JK, JS, KS and OGM. Field studies and data analysis were performed by KTPU, MRM, JK, KS, OGM, JS, JC, EW, AK-M, JM, MMc, and MM.

Competing Interests

The contact author has declared that none of the authors has any competing interests.

Acknowledgements and Financial Support

We thank the help of Dr. Jeremy Price from the United Kingdom Meteorological Office in operating the LIAISE field experiment, and Dr. Nicolas Jorgensen-Bambach from the United States Department of Agriculture Agricultural Research Service in Davis CA for his informal questions regarding the manuscript after the formal comment period closed. Portions of this research were funded by the United States Department of Agriculture National Institute of Food and Agriculture, Hatch Project CA-D-LAW-4526H, the California Department of Water Resources and the Sacramento-San Joaquin Delta Conservancy Delta Drought Response Pilot Program, the California Office of the Delta Watermaster, CALFED Bay-Delta Program, The PhD program of MRM was funded in part by the promotion of Jordi Vila to Professor of Meteorology at Wageningen University.

References

Beyrich, F., Richter, S.H., Weisensee, U., Kohsiek, W., Lohse, H., de Bruin, H.A.R., Foken, T, Goeckede, M., Berger, F., Vogt, R., Batchvarova, E. 2002. Experimental determination of turbulent fluxes over the heterogeneous LITFASS area: selected results from the LITFASS-98 experiment. Theor. Appl. Climatol. 73;19-34. DOI 10.1007/s00704-002-0691-7

Boone, A., Bellvert, J., Best, M., Brooke, J., Canut-Rocafort, G., Cuxart, J., Hartogensis, O., e Moigne, P., Miró, J. R., Polcher, J., Price, J., Quintana Seguí, P., & Wooster, M. (2021, December). Updates on the International Land Surface Interactions with the Atmophere over the Iberian Semi-Arid Environment (LIAISE) Field Campaign. *GEWEX News*, *31*(4), 17–21.

Bosveld, F.C., Beljaars, A.C.M. 2001. The impact of sampling rate on eddy-covariance flux estimates. Agricult. For. Meteorol. 109:39-45.

Brooke, J. K., Best, M. J., Lock, A. P., Osborne, S. R., Price, J., Cuxart, J., Boone, A., Canut-Rocafort, G., Hartogensis, O. K., & Roy, A. (2024). Irrigation contrasts through the morning transition. *Quarterly Journal of the Royal Meteorological Society*, *150*(758), 170–194. https://doi.org/10.1002/qj.4590

Foken, Th., Weisensee, U., Kirzel, H.-J., Thiermann, V., 1997: Comparison of new-type sonic

anemometers. Preprint volume of the 12th Symposium on Boundary Layers and turbulence,

28 July - 1 August 1997, Vancouver Canada, Am. Meteorol. Soc., Boston, 356-357.

Foken, T. 1999. Comparison of the sonic anemometer Young Model 81000 during VOITEX-99. Arbeitsergebnisse No. 8, Bayreuth, October 1999.

Frank, J.M., Massman, W.J., Ewers, B.E. 2013. Underestimates of sensible heat flux due to vertical velocity measurement errors in nonorthogonal sonic anemometers. Agric. For. Meteor. 171-172:72-81. . doi:10.1016/j.agrformet.2012.11.005.

Frank, J.M., Massman, W.J., Swiatek, E., Zimmerman, H.A., Ewers, B.E. 2016. All sonic anemometers need to correct for transducer and structural shadowing in their velocity measurements. J. Atmos. Ocean. Tech. 33:149-167. DOI: 10.1175/JTECH-D-15-0171.1

Frank J.M., Massman W.J., Chan W.S., Nowicki K., Rafkin S.C.R. 2020. Coordinate Rotation–Amplification in the Uncertainty and Bias in Non-orthogonal Sonic Anemometer Vertical Wind Speeds. Bound. Layer Meteorol. 2020;175:203–235. doi: 10.1007/s10546-020-00502-3

Haugen, D.A., Kaimal, J.C., Bradley, E.F. 1971. An experimental study of Reynolds stress and heat flux in the atmospheric surface layer. Quart. J.R. Met. Soc. 97:168-180.

Horst, T.W., Semmer, S.R., Maclean, G. 2015. Correction of a non-orthogonal, three-component sonic anemometer for flow distortion by transducer shadowing. Boundary-Layer Meteorol. 155:371-395. DOI 10.1007/s10546-015-0010-3

Horst, T.W., Vogt, R., Oncley, S.P. 2016. Measurements of flow distortion within the IRGASON integrated sonic anemometer and CO_2/H_2O gas analyzer. Boundary-Layer Meteorol. 160:1-15. DOI 10.1007/s10546-015-0123-8

Huq, S., De Roo, F., Foken, T., Mauder, M. 2017. Evaluation of probe-induced flow distortion of Campbell CSAT3 sonic anemometers by numerical simulation. Boundary-Layer Meteorol. 165:9-28. DOI 10.1007/s10546-017-0264-z

Kleissl, J., Meneveau, C., Parlange, M.B. 2003. On the magnitude and variability of subgrid-scale eddy-diffusion coefficients in the atmospheric surface layer. J Atmos. Sci. 60:2372-2388.

Kochendorfer, J. and Paw U, K.T., 2011. Field estimates of scalar advection across a canopy edge. Agric. Forest Meteorol., 151:585-594.: http://dx.doi.org/10.1016/j.agrformet.2011.01.003)

Kochendorfer, J., Meyers, T.P., Frank, J.M., Massman, W.J., Heuer, M.W. 2012. How well can e measure the vertical wind speed? Implication for fluxes of energy and mass. Boundary-Layer Meteorol. 145:383-398. doi:10.1007/s10546-012-9738-1

Lloyd, C. 2023. A path to successful eddy covariance measurements. https://uk-scape.ceh.ac.uk/sites/default/files/2023-09/Eddy%20Covariance%20Handbook-V21.pdf dowloaded August 4, 2024.

Loescher, H.W., Ocheltree, T., Tanner, B., Swiatek, E., Dano, B., Wong, J., Zimmerman, G., Campbell, J., Stock, C., Jacobsen, L., Shiga, Y., Kollas, J., Liburdy, J., Law, B.E. 2005. Comparison of temperature and wind statistics in contrasting environments among different sonic anemometer-thermometers. Agricult. For. Meteorol. 133: 119-138. doi:10.1016/j.agrformet.2005.08.009

Mangan, M. R., Hartogensis, O., Boone, A., Branch, O., Canut, G., Cuxart, J., de Boer, H. J., Le Page, M., Martínez-Villagrasa, D., Miró, J. R., Price, J., & Vilà-Guerau de Arellano, J. (2023). The surface-boundary layer connection across spatial scales of irrigation-driven thermal heterogeneity: An integrated data and modeling study of the LIAISE field campaign. *Agricultural and Forest Meteorology*, *335*, 109452. https://doi.org/10.1016/j.agrformet.2023.109452

Mauder, M., Oncley, S.P., Vogt, R., Weidinger, T., Ribeiro, L., Bernhofer, C., Foken, T., Kohsiek, W., Bruin, H.A.R.,Liu, H. 2007. The energy balance experiment EBEX-2000. Part II: Intercomparison of eddy-covariance sensors and post-field data processing methods. Boundary-Layer Meteorol. 123:29-54. doi:10.1007/s10546-006-9139-4

Mauder, M. 2013. A comment on "how well can we measure the vertical wind speed? Implications for fluxes or energy and mass" by Kochendorfer et al. Bondary-Layer Meteorol. 147:329-335. DOI 10.1007/s10546-012-9794-6

Mauder, M., Zeeman, M.J. 2018. Field intercomparison of prevailing sonic anemometers. Atmos. Meas. Tech. 11: 249-263. https://doi.org/10.5194/amt-11-249-2018

Merry, M. and Panofsky, H.A. 1976. Statistics of vertical motion over land and water. Quart. J. Royal Meteorol. Soc. 102: 255-260. https://doi.org/10.1002/qj.49710243120

Mortensen, N.G., Jojstrup, J. 1995. The Solent sonic-response and associated errors. Ninth Symposium on Meteorological Observations and Instrumentation, Preprints pp..501-506. American Meteorological Society, Boston, MA.

Nakai, T., Iwata, H., Harazono, Yl, Ueyama, M. 2014. An inter-comparisonn between Gill and Campbell sonic anemometers. Agricult For. Meteorol. 195-196:123-131.

Panofsky, H.A., Dutton, J.A. 1984. Atmosheric Turbulence. John Wiley & Sons 397pp.

Panofsky, H.A., Tennekes, H., Lenschow, D.., Wingaard, J.C. 1977. The characteristics of turbulent velocity components in the surface layer under convective conditions. Boundary-Layer Meteorol. 11:355-361.

Paw U, K.T., Baldocchi, D.D., Meyers, T. P., and Wilson, K., 2000. Correction of eddy-covariance measurements incorporating both advective effects and density fluxes. Boundary-layer Meteorol., 97:487-511

Paw U, K.T., Kent, E., Clay, J.M., Leinfelder-Miles, M., Lambert, J-J, McAuliffe, M., Edgar, D., Freiberg, S., Gong, R., Metz, M., Little, C., Temegsen, B. 2018. Appendix B. Field campaign report for water years 2015-2016 and 2016-2017. in A comparative study for estimating crop evapotranspiration in the Sacramento-San Joaquin Delta, report for the Office of the Delta Watermaster, University of California, Davis.

Paw U, K.T., Clay, J.M., McAuliffe, M., Schmiedeler, M., Mangan, M.R. 2019. Appendix B. Measuring evapotranspiration in fallow and cropped field sin the California Delta 2098-18. in Evapotranspiration of fallow field sin the California Delta. report for the Office of the Delta Watermaster, University of California, Davis.

Pena, A., Dellwik, E., Mann, J. 2019. A method to assess the accuracy of sonic anemometer measurements. Atmos. Meas. Tech. 12:237-252. doi.org/10.5194/amt-12-237-2019

Polonik, P., Chan, W.S., Billesbach, D.P., Burba, G., Li, J.,Nottrott, A., Bogoev, I., Conrad, B., Biraud, S.C. 2019. Comparison of gas analyzers for eddy covariance: effects of analyzer type and spectra correctdions on fluxes. Agricult. For. Meteorol. 272-273: 128-142.

Sharan, M., Gopalakrishnan, S.G. 1999. A local parameterization scheme for σ_w under stable conditions. J. Applied Meteorol. 38:617-622.

Thurtell, G.W., Tanner, C.B., Wesely, M.L. 1970. Three-dimensional pressure-sphere anemometer system. J. Applied. Meteorol. 9:379-385.

Wang, L., Lee, X., Wang, W., Wang, X., Wei, Z., Fu, C., Gao, Y., Lu, L., Song, W., Su, P., Lin, G. 2017. A meta-analysis of open-path eddy covariance observations of apparent CO_2 flux in cold conditions in FLUXNET. J. Atmos. Ocean. Tech. 34:2475-2487 DOI: 10.1175/JTECH-D-17-0085.1

Wyngaard, J.C., Cote, O.R., Izumi, Y. 1971. Local free convection, similarity, and the budgets of shear stess and heat flux. J. Atmos. Sci. 28:1171-1182.